



THE UNIVERSITY *of* EDINBURGH

Edinburgh Research Explorer

Real-time imaging of *Leishmania mexicana*-infected early phagosomes: a study using primary macrophages generated from green fluorescent protein-Rab5 transgenic mice

Citation for published version:

Lippuner, C, Paape, D, Paterou, A, Brand, J, Richardson, M, Smith, A, Hoffmann, K, Brinkmann, V, Blackburn, C & Aebischer, T 2009, 'Real-time imaging of *Leishmania mexicana*-infected early phagosomes: a study using primary macrophages generated from green fluorescent protein-Rab5 transgenic mice', *The FASEB Journal*, vol. 23, no. 2, pp. 483-491. <https://doi.org/10.1096/fj.08-108712>

Digital Object Identifier (DOI):

[10.1096/fj.08-108712](https://doi.org/10.1096/fj.08-108712)

Link:

[Link to publication record in Edinburgh Research Explorer](#)

Document Version:

Publisher's PDF, also known as Version of record

Published In:

The FASEB Journal

Publisher Rights Statement:

Freely available from Pub Med.

General rights

Copyright for the publications made accessible via the Edinburgh Research Explorer is retained by the author(s) and / or other copyright owners and it is a condition of accessing these publications that users recognise and abide by the legal requirements associated with these rights.

Take down policy

The University of Edinburgh has made every reasonable effort to ensure that Edinburgh Research Explorer content complies with UK legislation. If you believe that the public display of this file breaches copyright please contact openaccess@ed.ac.uk providing details, and we will remove access to the work immediately and investigate your claim.



Real-time imaging of *Leishmania mexicana*-infected early phagosomes: a study using primary macrophages generated from green fluorescent protein-Rab5 transgenic mice

Christoph Lippuner,^{*,1} Daniel Paape,^{*,‡} Athina Paterou,[‡] Janko Brand,^{*} Melville Richardson,[§] Andrew J. Smith,[§] Kirstin Hoffmann,^{*} Volker Brinkmann,[†] Clare Blackburn,[§] and Toni Aebischer^{*,‡,2}

^{*}Department of Molecular Biology and [†]Central Microscopy Unit, Max-Planck-Institute for Infection Biology, Berlin, Germany; and [‡]Marie Curie Team Pathogen Habitats, Institute of Immunology and Infection Research, and [§]Institute for Stem Cell Research, University of Edinburgh, Edinburgh, UK

ABSTRACT The small GTPase Rab5 is a key regulator of endosome/phagosome maturation and in intravesicular infections marks a phagosome stage at which decisions over pathogen replication or destruction are integrated. It is currently unclear whether *Leishmania*-infected phagosomes uniformly pass through a Rab5⁺ stage on their intracellular path to compartments with late endosomal/early lysosomal characteristics. Differences in routes and final compartments could have consequences for accessibility to antileishmanial drugs. Here, we generated a unique *gfp-rab5* transgenic mouse model to visualize Rab5 recruitment to early parasite-containing phagosomes in primary host cells. Using real-time fluorescence imaging of phagosomes carrying *Leishmania mexicana*, we determined that parasite-infested phagosomes follow a uniform sequence of transient Rab5 recruitment. Residence in Rab5⁺ compartments was much shorter compared with phagosomes harboring latex beads. Furthermore, a comparative analysis of parasite life-cycle stages and mutants deficient in *lpg1*, the gene encoding the enzyme required for synthesis of the dominant surface lipophosphoglycan, indicated that parasite surface ligands and host cell receptors modulate pathogen residence times in Rab5⁺ phagosomes, but, as far as tested, had no significant effect on intracellular *L. mexicana* survival or replication.—Lippuner, C., Paape, D., Paterou, A., Brand, J., Richardson, M., Smith, A. J., Hoffmann, K., Brinkmann, V., Blackburn, C., Aebischer, T. Real-time imaging of *Leishmania mexicana*-infected early phagosomes: a study using primary macrophages generated from green fluorescent protein-Rab5 transgenic mice. *FASEB J.* 23, 483–491 (2009)

Key Words: embryonic stem cells • inducible gene expression • doxycycline • wortmannin • reverse tetracycline transactivator • lipophosphoglycan

THE SMALL GTPASE RAB5 is recruited to early endocytic vesicles and in turn attracts numerous effector proteins,

such as Rabenosyn-5, Rabaptin-5, early endosomal antigen-1 (EEA1), and class I and III phosphatidylinositol 3-kinase (PI3K) regulatory subunits, into functional domains. These domains orchestrate endosome/phagosome maturation by organizing molecular machines involved in movement, cargo delivery, and membrane sorting, whereby vesicles undergo recycling or are directed to lysosomal compartments (1). Many intracellular pathogens taken up by phagocytosis (2–4) interfere with phagosome maturation at the Rab5⁺ stage to prevent being routed to lysosomes for destruction, e.g., *Mycobacterium tuberculosis* (5), *Listeria monocytogenes* (6), and *Leishmania donovani* (7, 8), often by affecting turnover of phosphatidylinositol phosphates (9). Thus, Rab5 marks a compartment in which decisions about pathogen survival or destruction are integrated (10). Recently, it was proposed that phagosome maturation is subject to higher-order signaling cascades as engaging Toll-like receptors (TLRs) accelerate the maturation of phagosomes containing TLR ligand-displaying particles (11, 12). This attractive hypothesis is debated, as others could not confirm these observations (13).

Leishmania spp. are medically relevant model pathogens (14). These protozoan parasites are transferred as promastigotes during a blood meal by their insect vectors and then are taken up by professional phagocytes wherein they transform into intracellular amastigotes (15). As for many other pathogens, on the basis of current data it is unclear whether *Leishmania*-containing phagosomes mature in a uniform way. For example, >60% of the parasites are located in Rab7⁺, transferrin

¹ Current address: Institut für Pharmazeutische Wissenschaften, Pharmazeutische Biologie und Biotechnologie, Albert-Ludwigs-Universität Freiburg, Germany.

² Correspondence: Marie Curie Team Pathogen Habitats, Institute of Immunology and Infection Research, University of Edinburgh, Edinburgh EH9 3JT, UK. E-mail: toni.aebischer@ed.ac.uk

doi: 10.1096/fj.08-108712

receptor-negative (TfR⁻)/EEA1-negative compartments within 10 min after phagocytosis, whereas a minority (<15%) is found in compartments positive for early and recycling endosome markers such as EEA1 (16, 17). Whether phagosomes expressing early and late endosomal markers, respectively, reflect a sequence in time or different habitat subpopulations is presently unclear. If they represent different habitats, this could have important implications. For example, the habitat subpopulations could have differential abilities to fuse with other vesicle populations. This could affect accessibility for drugs used to treat the infection. Moreover, the major phagocytic receptors involved in parasite uptake differ among life-cycle stages and vary depending on host immune status. It is unclear whether this affects the intracellular trafficking of the parasites or their survival.

Here, we report on the generation of a unique transgenic mouse model for the ubiquitous expression of functional fluorescent Rab5 at nontoxic levels to trace endocytic events and phagosome maturation in primary professional phagocytes. The mice harbor an *egfp-rab5* transgene under the control of the reverse tetracycline transactivator (18), allowing induction of green fluorescent protein (GFP)-Rab5 by doxycycline. Phagosome maturation was studied in GFP-Rab5-expressing bone marrow-derived macrophages (BMMΦs), which were infected with red fluorescent *Leishmania mexicana* parasites or exposed to latex beads. The system allowed us to study by real-time imaging whether early events in the maturation of parasite-containing phagosomes are uniform in primary cells, whether these are modulated by parasite surface ligand interaction with cognate receptors, and whether this would have consequences for the intracellular establishment of the parasite. Real-time recording unraveled a massive recruitment of Rab5 covering the entire phagosome membrane, which for parasites lasted only 1–2 min. Intriguingly, residence time in Rab5⁺ compartments was modulated by physiologically relevant major parasite surface ligand host cell receptor interactions. This result indicated that signaling cascades initiated by diverse host cell surface receptors indeed have an effect on phagosome maturation kinetics. However, this was not enough to change the ability of the parasite to establish productive intracellular infection.

MATERIALS AND METHODS

Chemicals and antibodies

Doxycycline was obtained from Clontech Laboratories Inc. (Palo Alto, CA, USA) and was dissolved at 20 mg/ml H₂O. Wortmannin was from Sigma-Aldrich Corp. (St. Louis, MO, USA) and was prepared as a 2 mM stock solution. Cy3-labeled transferrin was a kind gift from U. Schaible (Max-Planck-Institute for Infection Biology, Berlin, Germany). The Cy3-conjugated rat anti-mouse LAMP-1 antibody, 1D4B, was from BD Biosciences (San Jose, CA, USA); polyclonal rabbit anti-Rab5a antibodies were from Santa Cruz Biotechnology, Inc. (Santa Cruz, CA, USA), and secondary anti-rabbit antibodies

from goat conjugated to horseradish peroxidase (HRP) were from SouthernBiotech (Birmingham, AL, USA). Fluorescent latex beads were from Molecular Probes Inc. (Eugene, OR, USA).

Generation of transgenic embryonic stem (ES) cells and mice

E14TG2a cells (19) were grown in Glasgow minimal essential medium (Sigma-Aldrich Corp.) supplemented with 10% (v/v) fetal calf serum (FCS), 100 U/ml penicillin, 100 µg/ml streptomycin, and 2 mM L-glutamine, 1× nonessential amino acids, sodium pyruvate, 50 µM β-mercaptoethanol, and 100 U/ml human leukemia inhibitory factor (hLIF) (from culture supernatant of hLIF-transfected COS-7 cells). ES cells were grown on gelatinized tissue culture plasticware. Recombinant ES cells expressing doxycycline-inducible Rab5 protein fused to GFP were derived and characterized as described in Supplemental Material.

Chimeric mice were produced on the basis of protocols described previously by blastocyst injection (20). Offspring male founders were further bred to female C57BL/6 mice.

Parasite culture

L. mexicana mexicana (MNYC/BZ/62/M379) *lpg1*^{-/-} (21) and *L. mexicana mexicana* (MNYC/BZ/62/M379) *dsred14* (22) promastigotes were cultured *in vitro* in semidefined medium/10% heat inactivated FCS and 20 µg/ml hygromycin at 26°C. Amastigotes were cultured axenically at 34°C in Schneider's *Drosophila* medium (Life Technologies, Inc., Gaithersburg, MD, USA) supplemented with 10% heat-inactivated FCS and 3.9 g/l 2-(N-morpholino)ethanesulfonic acid (Sigma-Aldrich Corp.). Lipophosphoglycan (LPG)-deficient *L. mexicana* parasites were stained with SYTO 61 (Molecular Probes). Staining was performed on ice in medium with a 1:1000 SYTO 61 dilution. Amastigotes were singularized before staining. After 20 min, the parasites were centrifuged and resuspended in fresh medium and were then cultured further.

Derivation of BMMΦs and dendritic cells

Bone marrow cells were harvested from female mice and plated at 5 × 10⁶ cells/100 mm bacterial Petri dish in 15 ml of DMEM supplemented with 10% FCS, 2 mM glutamine, and macrophage colony-stimulating factor (M-CSF) (20% L929 cell-conditioned culture supernatant). On day 6 of culture, nonadherent cells were washed away, and the BMMΦs were released from the plastic by incubation at 37°C with PBS. BMMΦs were replated in the same medium at the required density on µ-slides (Ibidi GmbH, München, Germany) and were used the following day. Bone marrow-derived dendritic cells were produced as described previously (23).

Flow cytometry

Cells were fixed with 4% paraformaldehyde (PFA) for 15 min and were then analyzed on a Becton Dickinson FACSsort (Becton Dickinson, Franklin Lakes, NJ, USA). Green fluorescence signals were detected in FL-1. Cell debris and dead cells were excluded from the analysis on the basis of forward- and side-scatter characteristics, and 10⁴ to 2 × 10⁴ events were recorded. Fluorescence-activated cell sorting data were analyzed using CellQuest (version 3.3; BD Biosciences) or FCS express version 2 (De Novo Software, Los Angeles, CA, USA).

Western blot analysis

Wild-type (WT) and *gfp-rab5* transgenic ES cells were washed with PBS and subsequently lysed in SDS-PAGE sample buffer. Proteins were separated by SDS-PAGE, transferred onto polyvinylidene difluoride membranes, and probed with a rabbit polyclonal antibody against Rab5a. After incubation with HRP-conjugated secondary antibodies, the blots were developed by enhanced chemiluminescence (Western Lightening-Chemiluminescence Reagent Plus; PerkinElmer Life and Analytical Sciences, Inc., Wellesley, MA, USA) and exposed to film (Hyperfilm; Amersham Bioscience Corp., Piscataway, NJ, USA).

Immunofluorescence analysis of fixed cells and mouse tissues

To determine the relative distribution of Rab5, ES cells were grown on glass coverslips and induced to spontaneously differentiate in the presence of 2 $\mu\text{g}/\text{ml}$ doxycycline. The distribution of GFP-Rab5 was studied in relation to LAMP-1 and transferrin. Therefore, cells were either starved from serum for 1 h or were incubated with 10 $\mu\text{g}/\text{ml}$ Cy3-labeled transferrin (kind gift of U. Schaible) for 15 min and then were fixed with 4% HEPES-buffered PFA for 30 min or fixed directly, permeabilized, and stained with anti-LAMP-1 antibodies (22). Optionally, cells were treated for 120 min with 100 nM wortmannin before the experiment. For results, see Supplemental Material.

Different mouse tissues were collected from mice treated or not treated with doxycycline and fixed for 6 h in 2% PFA in PBS. Fixed tissues were washed, equilibrated overnight in PBS/30% sucrose, embedded in optimal cutting temperature (O.C.T.) compound (Vogel Medizinische Technik und Elektronik, Giessen, Germany) and frozen. Sections (10 μm) were cut, air-dried at room temperature, and stored at -70°C . Sections were thawed, and nuclei were stained with 1 $\mu\text{g}/\text{ml}$ 4,6-diamidino-2-phenylindole (DAPI) in Tris-buffered saline/0.5% Tween 20 for 10 min.

Cells and tissues were finally mounted in Mowiol. Pictures were captured with a Leica DMR fluorescence microscope (Leica, Wetzlar, Germany) using a Nikon digital camera DXM1200 (Nikon, Melville, NY, USA) and ACT software (version 2.00; Leica). Pseudocolor was applied with Adobe Photoshop software (Adobe Systems, San Jose, CA, USA). Contrast and brightness enhancement of acquired images was also performed with Adobe Photoshop software to enhance weak fluorescence of some images and to improve the contrast.

Epifluorescence pictures were analyzed for fluorescent signal overlap by visual inspection. With the use of Adobe Photoshop, a grid was projected onto the image of a given cell, all fluorescent structures in a grid square were examined for green and red fluorescence, and colocalization grid squares were chosen to ensure that peripheral and perinuclear structures were represented. At least 8 cells were analyzed, counting >80 single fluorescent structures per cell.

Live cell imaging

BMM Φ s were grown on μ -slides. Parasites were added, and time-lapse image series were acquired at 37°C and 5% CO_2 on an inverted Zeiss Axiovert 200M microscope equipped with an $\times 100$ oil-immersion objective. Image collection was controlled by Open Lab software (version 4.0.3; Open Lab, Florence, Italy).

Each individual cinematic image series was processed manually with Open Lab software and ImageJ (version 1.33u; National Institutes of Health, Bethesda, MD, USA) to assess

Rab5 recruitment and loss. Data were analyzed using GraphPad Prism 3.1 statistics software (GraphPad Software Inc., San Diego, CA, USA).

Determination of replication competent parasites from infected BMM Φ s

C57BL/6 female BMM Φ s were seeded on 96-well TC plates at 4×10^4 cells/well. After the cells had attached, the medium was removed and replaced with fresh medium with or without 100 nM wortmannin (Sigma-Aldrich Corp.) for 2 h. Then cells were infected with stationary cultures of promastigotes of *L. mexicana* of WT and *lpg* $^{-/-}$ genetic background (clone I8D; cf. ref. 21) at multiplicity of infection of 5:1 in triplicates, spun for 10 min at 700 g, and incubated for 30 min at 34°C to allow infection. Free parasites were washed away, and fresh medium was added to the infected macrophages, which were incubated for a further 24, 48, 72, and 96 h. Time 0 denoted the point at which the parasites were washed away. At each time point macrophages were lysed in DMEM/0.008% SDS to isolate the internalized parasites, and the lysate was diluted 1:10 and 1:100 in semidefined minimal (SDM) medium and incubated at 26°C . Promastigotes were enumerated at day 3–6 to confirm linear growth, and numbers at day 4 were used to compare treatments.

RESULTS

Derivation of *gfp-rab5* transgenic mice and transgene induction in diverse tissues

Having established a system for inducible GFP-Rab expression on the basis of integration into the X chromosomal *hprt* locus that reports correctly in ES cells (cf. Supplemental Material), lines of transgenic mice were produced by blastocyst injection. Male chimeras were obtained and bred to C57BL/6 female mice. Litters were of normal size, indicating that the transgene is compatible with normal development. Transgenic offspring were identified by polymerase chain reaction, and transgene-carrying, heterozygous females were treated on consecutive days with intraperitoneal injections of doxycycline. Expression of GFP-Rab5 protein was then assessed on cryosections prepared from diverse tissues. Consistent with *hprt* being an open locus in most cell types, GFP-Rab5 was detected in all tissues tested (Fig. 1). No signal was detected in vehicle-treated, transgenic mice, indicating tight regulation of gene expression.

Next, we derived macrophages and dendritic cells from bone marrow of heterozygous transgenic females by culture for 7 days in M-CSF or granulocyte-macrophage CSF-containing medium, respectively. GFP-Rab5 expression was induced by adding doxycycline either throughout the 7 days or only for the last 2 days. GFP-Rab5 was expressed by up to 37% of the heterozygous cells, independent of the protocol used. Cell yield and morphology were not different from nontransgenic BMM Φ or dendritic cells (not shown) indicating that transgene induction did not compromise cell proliferation, differentiation, or viability. The distribution of the fluorescence recapitulated the results ob-

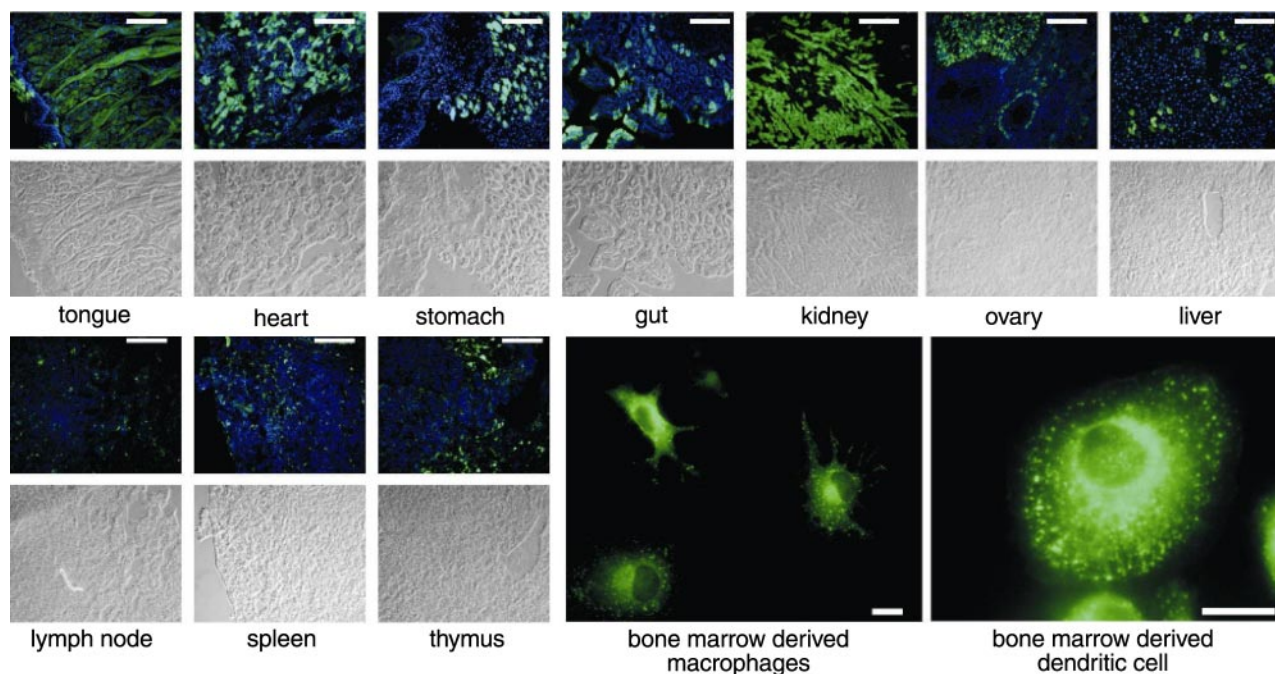


Figure 1. GFP-Rab5 expression is broadly inducible in tissues of transgenic mice. Mice heterozygote for *gfp-rab5* fusion gene were treated for 3 days with daily i.p. injections of 3 mg of doxycycline. Images show fluorescence (top: blue, DAPI; green, GFP-Rab5) and light micrographs (bottom) of different tissues and bone marrow-derived macrophages and dendritic cells, recorded through $\times 20$ objective for tissues and $\times 100$ objective for BMM Φ and dendritic cells. Scale bars = 100 μm (tissues); 10 μm (cells).

tained with the ES cell lines (compare Supplemental Fig. 2 and Fig. 1). This indicated that GFP-Rab5 proteins labeling the early endosomal compartment could be expressed in primary professional phagocytes.

Kinetics of GFP-Rab5 recruitment and loss from phagosomes containing different cargo

The maturation of phagosomes is difficult to assess because of the asynchronous nature of particle uptake or infection with pathogens. Thus, live cell imaging of GFP-Rab5 expressing transgenic primary phagocytes was used to visualize the fate of individual phagosomes. By using this system, kinetics of phagosome maturation can be divided in a pre-Rab5⁺ phase, a phase that is Rab5⁺, and a phase that has lost Rab5.

To evaluate our model and for comparative reasons as well as for reference to published data, we monitored the uptake of latex beads and maturation of bead-containing phagosome maturation. BMM Φ s were treated with doxycycline and then incubated with carboxylated red fluorescent latex beads (1 μm diameter). Beads and phagosomes were analyzed in real time by epifluorescence microscopy. Intervals of 45–70 min were monitored at 6 frames/min. Beads were readily taken up, and bead-containing phagosomes recruited GFP-Rab5 within 50–70 s (not shown). These compartments retained GFP-Rab5 on average for >30 min (Fig. 2). This is a lower estimate of the residence time in GFP-Rab5⁺ compartments because bead-containing phagosomes could move out of focus. Pretreatment of the BMM Φ s with wortmannin for 2 h to inhibit PI3Ks and

“freeze” phagosome at the early endosome stage induced giant endosomes as expected but had no effect on GFP-Rab5 recruitment or loss. These findings agree with published data on latex bead phagocytosis (24) and the effect of wortmannin (25), indicating faithful and proper reporting of the GFP-Rab5 transgene.

We next investigated the paths of phagosomes containing *L. mexicana*, a real pathogen. BMM Φ s engulfed the parasites, and phagosomes were moved from the site of uptake toward the perinuclear area (*cf.* Supplemental Movie 2). During this process, parasite-containing phagosomes recruited GFP-Rab5 within the first minute after uptake, resulting in strikingly uniform distribution of Rab5 over the phagosome membrane. In contrast to bead-containing vesicles, GFP-Rab5 recruitment was very transient, and the GTPase disappeared from the phagosome after an average time of <2 min (median 100 s, range 20–280 s (Figs. 3 and 4; see also Supplemental Movie 2). Importantly, the sequence of events was the same for every single phagosome observed, indicating uniform but dramatically different kinetics of Rab5 loss of pathogen-containing phagosomes compared with bead-containing phagosomes (Fig. 2).

Occasionally, homotypic fusion of individual parasite-containing phagosomes was observed at the GFP-Rab5⁺ stage in cells that had phagocytosed multiple parasites (not shown). It is noteworthy that in these cases GFP-Rab5 was remaining for extended times on the phagosome, reminiscent of the behavior of latex bead carrying compartments. Fusions of GFP-Rab5⁺

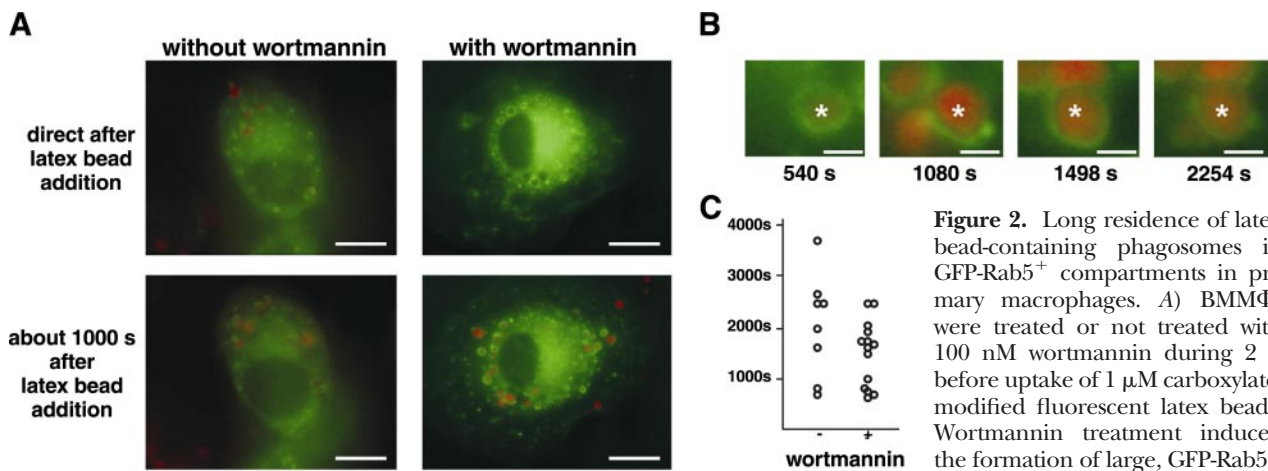


Figure 2. Long residence of latex bead-containing phagosomes in GFP-Rab5⁺ compartments in primary macrophages. **A)** BMMΦs were treated or not treated with 100 nM wortmannin during 2 h before uptake of 1 μM carboxylate-modified fluorescent latex beads. Wortmannin treatment induced the formation of large, GFP-Rab5⁺ endosomes. Images acquired from

control cells or wortmannin-treated cells. **B)** Still images of a track of a representative bead-containing vesicle over time. **C)** Quantitative analysis of bead residence intervals in Rab5⁺ vesicles. Scale bars = 10 μm (**A**); 1 μm (**B**).

phagosomes containing a parasite with parasite-containing phagosomes that had passed this stage was never observed.

Influence of promastigote surface ligand-host cell receptor interactions on phagosome maturation

Host phagocytes encounter *Leishmania* in two forms during infection: the vector-transmitted, extracellular promastigotes and the host-borne amastigotes. For the uptake of promastigotes, LPG is a prominent ligand (26) because it covers the surface, forming a glycocalyx, and engages complement receptor 3 (CR3) (27), triggering uptake. Thus, we infected GFP-Rab5⁺ BMMΦs with LPG-expressing, red fluorescent *L. mexicana* promastigotes (22) and with LPG-deficient mutant promastigotes (21) labeled with the red fluorescent DNA dye SYTO 61 to investigate a potential role of the major parasite surface ligand on phagosome maturation. The BMMΦs phagocytosed both parasite forms and, as shown above, all phagosomes independent of the parasite strain they contained underwent Rab5 recruitment and subsequent loss. Real-time tracking showed that LPG-deficient parasites lacking this dominant surface ligand resided significantly longer in GFP-Rab5⁺ vesicles (Fig. 4, left panel; median 150 s, range 20–290 s; $P < 0.05$).

In chronically infected or immune hosts, parasites become opsonized with antibodies (28). Therefore, physiological relevance is thought to shift from CR3- to Fcγ receptor (FcγR)-mediated phagocytosis (29–31). To model this shift and mimic infection in, e.g., a vaccinated host, promastigotes were opsonized with serum immunoglobulin (Ig) from infected mice under conditions in which complement activation is minimal to enforce FcγR interactions. Ig-opsonized parasites were readily phagocytosed. Under these conditions, residence in GFP-Rab5⁺ vesicles was significantly extended in comparison to WT, nonopsonized promastigotes with a median residence time of 180 s ($P < 0.05$).

Kinetics of Rab5 recruitment to *L. mexicana* amastigote-containing phagosomes

Amastigote forms of *L. mexicana* can be cultured, and we used such axenic amastigotes of both WT and LPG-deficient parasites to infect host cells and determined the kinetics of phagosome maturation for this life-cycle stage. As shown in Fig. 4 (right panel), amastigotes showed kinetics of Rab5 recruitment and loss that were very similar to those of promastigotes. Moreover, no significant difference was observed between WT and mutant amastigotes. Because this life-cycle form does not synthesize LPG or the other major promastigote surface molecule contributing to macrophage binding, glycoprotein gp63 (32–34), this confirmed that differences noted at the promastigote stage were not due to other, unknown characteristics that may have arisen during cloning of the mutant line.

Modulation of residence time in the Rab5⁺ compartment did not alter parasite infection success

It has been shown for *L. donovani* that LPG delays phagosome maturation (8) and that Rab5 is relevant for the leishmanicidal functions of the host cell (7). Hence, altered residence times in Rab5⁺ compartments might have an effect on intracellular survival. We therefore determined survival and replication of wild type and *lpg1*^{-/-} promastigotes in macrophages. In addition, we used wortmannin pretreatment, which delays phagosome maturation and extends residence time in Rab5 compartments, to assess the effect this might have on intracellular parasite survival and intracellular growth (Fig. 5). Numbers of live, mutant *lpg1*^{-/-} *L. mexicana* promastigotes dropped faster than those of WT parasites during the first 48 h of infection, but subsequent growth of the surviving parasites was also faster, resulting in no significant net effect. Wortmannin pretreatment of host cells to delay phagosome maturation experimentally had no significant effect on

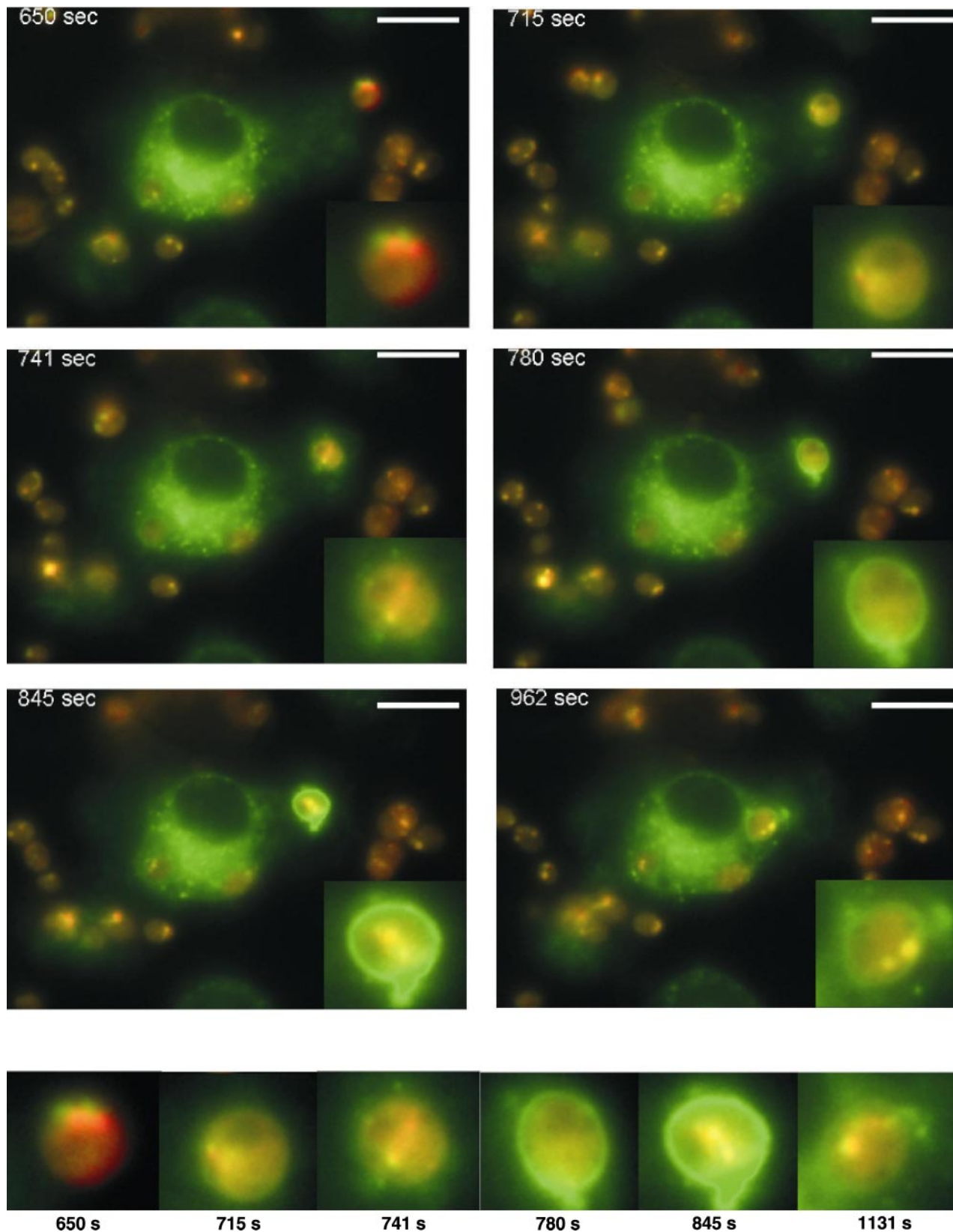


Figure 3. Sequence of entry, residence, and exit of *L. mexicana* into Rab5⁺ compartments in primary BMMΦs. Top panel: still images of cinematic analyses of uptake of red fluorescent *L. mexicana* amastigote parasites by BMMΦs. Time of picture recording is indicated; sequence runs from top left to bottom right. The uptake of one parasite into a cell that has already phagocytosed two other parasites is shown. Arrows locate the phagosome that is traced over time; insets show the respective area enlarged. The nascent phagosome is initially GFP-Rab5⁻ and then becomes positive, and fusion with GFP-Rab5⁺ endosomes is concomitantly observed. The *Leishmania*-containing phagosome moved toward the nucleus during maturation and lost GFP-Rab5. Scale bars = 10 μ m. Bottom panel: snapshots of time trace of the monitored phagosome.

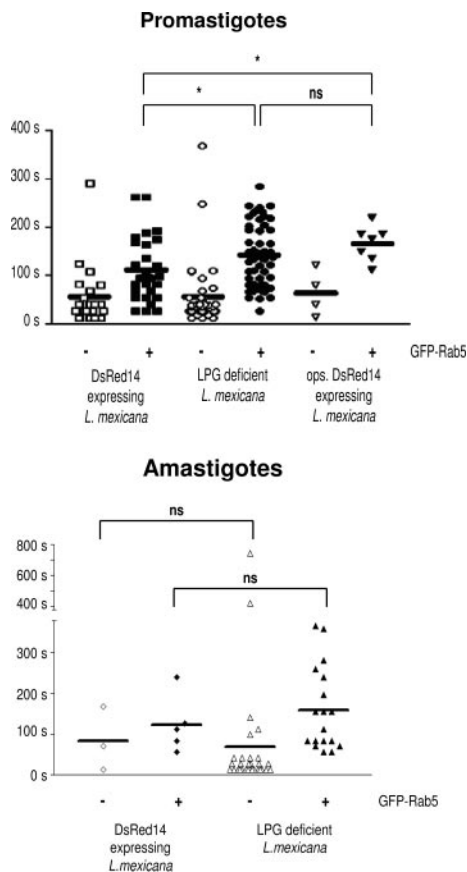


Figure 4. Residence times in Rab5⁺ compartments vary, depending on dominant parasite surface ligands. *A*) Time in pre-Rab5 and Rab5⁺ compartments (open and solid symbols, respectively) of *L. mexicana* LPG-expressing WT promastigotes (squares) and mutant *lpgI*^{-/-} promastigotes (circles) and serum Ig-opsonized (Ig-ops.; triangles) WT *L. mexicana* promastigotes. *B*) Times of *L. mexicana* WT (diamonds) and mutant *lpgI*^{-/-} (triangles) amastigotes in pre-Rab5 and Rab5⁺ compartments (open and solid symbols, respectively) are indicated. Each dot represents cinematic analysis of the trace of an individual phagosome. **P* < 0.05, WT *vs.* mutant parasites; 2-sided Student's *t* test. ns, nonsignificant.

survival or subsequent growth of either WT or mutant *L. mexicana* promastigotes.

DISCUSSION

We have developed a unique inducible GFP-Rab5 transgenic mouse model to visualize Rab5 recruitment to endocytic vesicles. This approach enabled us to resolve the first minutes of maturation of *Leishmania*-infected phagosomes in primary macrophages despite the fact that infection is not synchronous. Our results establish that all parasite-containing phagosomes follow a uniform early maturation sequence and pass through a Rab5⁺ compartment in primary host cells.

Because *Leishmania* life-cycle stages differ in their surface ligands and physiological relevance of phagocytic receptors, *e.g.*, CR3 and FcγR, depends on the immune status of the host, our model system and

available mutant parasites allowed us to investigate the influence of dominant ligand receptor pairs on the kinetics of Rab5 recruitment to and loss from phagosomes. Phagosome formation requires local F-actin assembly (35) that was shown to peak between 10 and ~100 s after cognate contact with model beads (36, 37). The duration of the pre-Rab5 stage for parasite-containing vesicles was between these limits. The mechanism of initial Rab5 recruitment to phagosomes is unclear, but the cinematic sequences suggested that part of the Rab5 stemmed from homotypic fusion events with already GFP-Rab5⁺ vesicles. EEA-1 may be involved in that process (38), as it can tether early endosomes to newly formed Rab5⁺ phagosomes. A homotypic fusion mechanism also explains the few fusion events observed between parasite-containing GFP-Rab5⁺ phagosomes. Our comparative data on the kinetics of Rab5 recruitment and loss on bead- and pathogen-containing phagosomes confirmed that that type of cargo can have a dramatic effect on the behavior of the phagosome. Our data also agree with evidence that higher order signaling cascades are implicated in modulating endosome/phagosome maturation (39). Ligand-receptor interactions acting during parasite binding and phagosome formation clearly modulated median residence times in Rab5⁺ compartments, whereas the duration of the pre-Rab5 stage was not affected. Absence of LPG, the dominant ligand on promastigotes, increased these intervals. LPG coats promastigotes entirely, engages CR3 directly (27, 40), and triggers CR3-mediated phagocytosis (41), but, at least in dendritic cells, can induce a proinflammatory response (42) and on mac-

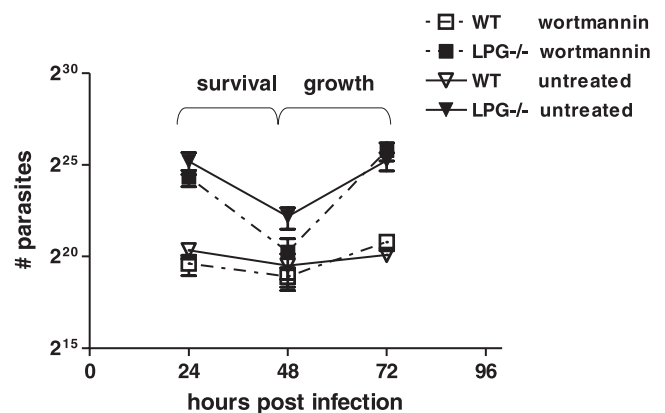


Figure 5. Modulation of phagosome maturation by LPG or reversible wortmannin treatment does not affect infection success of *L. mexicana* promastigotes in BMMΦs. Cells were treated or not treated with 100 nM wortmannin for 2 h and then infected with *L. mexicana* *lpgI*^{-/-} or WT promastigotes for 30 min. Parasites and wortmannin were washed away, and infected cells were further incubated as indicated. Live intracellular parasites were enumerated by lysis of host cells and growth in SDM medium. Values represent parasite numbers derived from BMMΦs infected for 24, 48, and 72 h. Survival and growth were analyzed and are represented as the mean difference of parasite numbers at 24 *vs.* 48 h infection and 48 *vs.* 72 h, respectively. Both phases of infection were not affected by wortmannin (unpaired Student's *t* test; *P* > 0.05; *n* = 6; error bars = SE).

rophages was shown to interact with TLR-2 (43, 44). TLR signaling pathways reportedly affect phagosome maturation (12), although this view has since been challenged (45). The absence of LPG had a statistically significant effect on residence times of *L. mexicana* promastigotes in Rab5⁺ compartments, but the relevance of this result seems to differ between species. For cultured *L. donovani* promastigotes, LPG was shown to delay phagosome maturation and benefit parasite survival in model host cells (7, 8), our results show that it did not significantly affect the net success of *L. mexicana* promastigotes in nonactivated, primary host cells. It will be interesting to determine the reasons for this.

Of note, LPG- or opsonization-mediated modulation of residence in Rab5⁺ compartments overlaid an even broader variation within a population of phagosomes formed by taking up parasites of the same kind. Particle shape has been shown to have a dramatic effect on phagocytosis (46). *Leishmania* are anisotropic; hence the number of receptor ligand systems binding to a single parasite and triggering phagocytosis may be very different between a parasite docking to a host cell only with the tip of its body *vs.* one that is interacting over a greater surface. In these situations differences in signal strengths emanating from host cell surface receptors may be generated, and this may explain part of the variation in maturation kinetics. We are currently investigating this hypothesis.

Residence times of Ig-opsonized parasites in Rab5⁺ compartments were 5 times shorter than those reported for Ig-opsonized sheep red blood cells in GFP-Rab5-transfected RAW cells (47). RAW cells are macrophage-like cells but, based on microarrays, display numerous differences to primary macrophages (48). Thus, the divergent residence times may reflect functional differences between RAW and primary macrophage cells. Alternatively, the exposure of RAW cells to plasmid DNA during transfection/electroporation to induce transgene expression could have an effect on maturation kinetics because the plasmid vector DNA contains sequences that can trigger TLR-9 (49).

The application of functional Rab fusion proteins in professional phagocytes has generally met with limited success because these cells are difficult to manipulate genetically and often become activated by the respective procedures (12, 50, 51). Furthermore, expression in transfected cells is difficult to control and overexpression, *e.g.*, of Rab5, can be toxic and can alter vesicular dynamics (52). The system described here, however, appears not to be subject to these caveats. GFP-Rab5 induced in primary cells was easily detected, faithfully reflected the dynamics of endogenous *rab5*, and showed no toxicity. Preliminary data with *gfp-rab7* or *tfr-gfp* transgenic ES cells suggested that the approach can be extended to other vesicle subpopulations (unpublished results). Furthermore, the two-component TET-ON system was adapted so that the system behaves like a single X chromosomally inherited trait opening the attractive avenue to mobilize it easily into the background of mutant mice with genetic defects in

phagocytosis/endocytosis (53, 54) or other related processes.

In summary, we report on the generation of a unique *gfp-rab5* transgenic mouse model to study phagocytosis and endocytosis in diverse primary cell types. Here, we used it to establish the uniform sequence of entry and exit for *Leishmania*-containing phagosomes into Rab5 compartments and to determine with high temporal resolution residence intervals that we show are influenced by early cell surface receptor-parasite ligand interactions. FJ

We thank J. Nichols for blastocyst injections; S. Moese (Max Planck Institute for Infection Biology, Berlin, Germany), S. Bronson (University of North Carolina, Chapel Hill, NC, USA), A. Galmiche (Max Planck Institute for Infection Biology), D. Colby (University of Edinburgh, Edinburgh, UK), and D. Hills (University of Edinburgh) for DNA constructs and reagents; U. Klemm for continuous advice on ES cell cultures; and U. Schaible and M. Drab for helpful comments on the manuscript. The study was supported by grants from the Deutsche Forschungsgemeinschaft (Ae16/3-1) and the European Molecular Biology Organization (ASTF 171-2002) and by a Marie Curie Excellence Award to T.A. C.L. was supported by the Boehringer Ingelheim Foundation. Finally, we also acknowledge the continuous support of T. F. Meyer. The authors have no conflicting commercial interests.

REFERENCES

1. Zerial, M., and McBride, H. (2001) Rab proteins as membrane organizers. *Nat. Rev. Mol. Cell Biol.* **2**, 107–117
2. Aderem, A., and Underhill, D. M. (1999) Mechanisms of phagocytosis in macrophages. *Annu. Rev. Immunol.* **17**, 593–623
3. Aderem, A. (2003) Phagocytosis and the inflammatory response. *J. Infect. Dis.* **187**, S340–S345
4. Stuart, L. M., and Ezekowitz, R. A. (2005) Phagocytosis: elegant complexity. *Immunity* **22**, 539–550
5. Fratti, R. A., Backer, J. M., Gruenberg, J., Corvera, S., and Deretic, V. (2001) Role of phosphatidylinositol 3-kinase and Rab5 effectors in phagosomal biogenesis and mycobacterial phagosome maturation arrest. *J. Cell Biol.* **154**, 631–644
6. Alvarez-Dominguez, C., and Stahl, P. D. (1999) Increased expression of Rab5a correlates directly with accelerated maturation of *Listeria monocytogenes* phagosomes. *J. Biol. Chem.* **274**, 11459–11462
7. Duclos, S., and Desjardins, M. (2000) Subversion of a young phagosome: the survival strategies of intracellular pathogens. *Cell. Microbiol.* **2**, 365–377
8. Lodge, R., and Descoteaux, A. (2005) Modulation of phagolysosome biogenesis by the lipophosphoglycan of *Leishmania*. *Clin. Immunol.* **114**, 256–265
9. Pizarro-Cerda, J., and Cossart, P. (2004) Subversion of phosphoinositide metabolism by intracellular bacterial pathogens. *Nat. Cell Biol.* **6**, 1026–1033
10. Scott, C. C., Botelho, R. J., and Grinstein, S. (2003) Phagosome maturation: a few bugs in the system. *J. Membr. Biol.* **193**, 137–152
11. Blander, J. M., and Medzhitov, R. (2006) Toll-dependent selection of microbial antigens for presentation by dendritic cells. *Nature* **440**, 808–812
12. Blander, J. M., and Medzhitov, R. (2004) Regulation of phagosome maturation by signals from Toll-like receptors. *Science* **304**, 1014–1018
13. Russell, D. G., and Yates, R. M. (2007) TLR signalling and phagosome maturation: an alternative viewpoint. *Cell. Microbiol.* **9**, 849–850
14. Herwaldt, B. L. (1999) *Leishmaniasis*. *Lancet* **354**, 1191–1199

15. Antoine, J. C., Prina, E., Courret, N., and Lang, T. (2004) *Leishmania* spp.: on the interactions they establish with antigen-presenting cells of their mammalian hosts. *Adv. Parasitol.* **58**, 1–68
16. Antoine, J. C., Prina, E., Lang, T., and Courret, N. (1998) The biogenesis and properties of the parasitophorous vacuoles that harbour *Leishmania* in murine macrophages. *Trends Microbiol.* **6**, 392–401
17. Courret, N., Frehel, C., Gouhier, N., Pouchelet, M., Prina, E., Roux, P., and Antoine, J. C. (2002) Biogenesis of *Leishmania*-harbouring parasitophorous vacuoles following phagocytosis of the metacyclic promastigote or amastigote stages of the parasites. *J. Cell Sci.* **115**, 2303–2316
18. Gossen, M., Freundlieb, S., Bender, G., Muller, G., Hillen, W., and Bujard, H. (1995) Transcriptional activation by tetracyclines in mammalian cells. *Science* **268**, 1766–1769
19. Thompson, S., Clarke, A. R., Pow, A. M., Hooper, M. L., and Melton, D. W. (1989) Germ line transmission and expression of a corrected HPRT gene produced by gene targeting in embryonic stem cells. *Cell* **56**, 313–321
20. Bradley, A., Evans, M., Kaufman, M. H., and Robertson, E. (1984) Formation of germ-line chimaeras from embryo-derived teratocarcinoma cell lines. *Nature* **309**, 255–256
21. Ilg, T. (2000) Lipophosphoglycan is not required for infection of macrophages or mice by *Leishmania mexicana*. *EMBO J.* **19**, 1953–1962
22. Sorensen, M., Lippuner, C., Kaiser, T., Misslitz, A., Aebischer, T., and Bumann, D. (2003) Rapidly maturing red fluorescent protein variants with strongly enhanced brightness in bacteria. *FEBS Lett.* **552**, 110–114
23. Bennett, C. L., Misslitz, A., Colledge, L., Aebischer, T., and Blackburn, C. C. (2001) Silent infection of bone marrow-derived dendritic cells by *Leishmania mexicana* amastigotes. *Eur. J. Immunol.* **31**, 876–883
24. Desjardins, M., Huber, L. A., Parton, R. G., and Griffiths, G. (1994) Biogenesis of phagolysosomes proceeds through a sequential series of interactions with the endocytic apparatus. *J. Cell Biol.* **124**, 677–688
25. Vieira, O. V., Bucci, C., Harrison, R. E., Trimble, W. S., Lanzetti, L., Gruenberg, J., Schreiber, A. D., Stahl, P. D., and Grinstein, S. (2003) Modulation of Rab5 and Rab7 recruitment to phagosomes by phosphatidylinositol 3-kinase. *Mol. Cell Biol.* **23**, 2501–2514
26. Handman, E., and Goding, J. W. (1985) The *Leishmania* receptor for macrophages is a lipid-containing glycoconjugate. *EMBO J.* **4**, 329–336
27. Talamas-Rohana, P., Wright, S. D., Lennartz, M. R., and Russell, D. G. (1990) Lipophosphoglycan from *Leishmania mexicana* promastigotes binds to members of the CR3, p150,95 and LFA-1 family of leukocyte integrins. *J. Immunol.* **144**, 4817–4824
28. Guy, R. A., and Belosevic, M. (1993) Comparison of receptors required for entry of *Leishmania major* amastigotes into macrophages. *Infect. Immun.* **61**, 1553–1558
29. Peters, C., Aebischer, T., Stierhof, Y. D., Fuchs, M., and Overath, P. (1995) The role of macrophage receptors in adhesion and uptake of *Leishmania mexicana* amastigotes. *J. Cell Sci.* **108**, 3715–3724
30. Kima, P. E., Constant, S. L., Hannum, L., Colmenares, M., Lee, K. S., Haberman, A. M., Shlomchik, M. J., and McMahon-Pratt, D. (2000) Internalization of *Leishmania mexicana* amastigotes via the Fc receptor is required to sustain infection in murine cutaneous leishmaniasis. *J. Exp. Med.* **191**, 1063–1068
31. Morehead, J., Coppens, I., and Andrews, N. W. (2002) Opsonization modulates Rac-1 activation during cell entry by *Leishmania amazonensis*. *Infect. Immun.* **70**, 4571–4580
32. Russell, D. G., and Wilhelm, H. (1986) The involvement of the major surface glycoprotein (gp63) of *Leishmania* promastigotes in attachment to macrophages. *J. Immunol.* **136**, 2613–2620
33. Bahr, V., Stierhof, Y. D., Ilg, T., Demar, M., Quinten, M., and Overath, P. (1993) Expression of lipophosphoglycan, high-molecular weight phosphoglycan and glycoprotein 63 in promastigotes and amastigotes of *Leishmania mexicana*. *Mol. Biochem. Parasitol.* **58**, 107–121
34. Yao, C., Donelson, J. E., and Wilson, M. E. (2003) The major surface protease (MSP or GP63) of *Leishmania* sp. Biosynthesis, regulation of expression, and function. *Mol. Biochem. Parasitol.* **132**, 1–16
35. Love, D. C., Mentink, K. M., and Mosser, D. M. (1998) *Leishmania amazonensis*: the phagocytosis of amastigotes by macrophages. *Exp. Parasitol.* **88**, 161–171
36. Defacque, H., Egeberg, M., Habermann, A., Diakonova, M., Roy, C., Mangeat, P., Voelter, W., Marriott, G., Pfannstiel, J., Faulstich, H., and Griffiths, G. (2000) Involvement of ezrin/moesin in de novo actin assembly on phagosomal membranes. *EMBO J.* **19**, 199–212
37. Scott, C. C., Dobson, W., Botelho, R. J., Coady-Osberg, N., Chavrier, P., Knecht, D. A., Heath, C., Stahl, P., and Grinstein, S. (2005) Phosphatidylinositol-4,5-bisphosphate hydrolysis directs actin remodeling during phagocytosis. *J. Cell Biol.* **169**, 139–149
38. Stephens, L., Ellison, C., and Hawkins, P. (2002) Roles of PI3Ks in leukocyte chemotaxis and phagocytosis. *Curr. Opin. Cell Biol.* **14**, 203–213
39. Pelkmans, L., Fava, E., Grabner, H., Hannus, M., Habermann, B., Krausz, E., and Zerial, M. (2005) Genome-wide analysis of human kinases in clathrin- and caveolae/raft-mediated endocytosis. *Nature* **436**, 78–86
40. Russell, D. G. (1987) The macrophage-attachment glycoprotein gp63 is the predominant C3-acceptor site on *Leishmania mexicana* promastigotes. *Eur. J. Biochem.* **164**, 213–221
41. Blackwell, J. M. (1985) Role of macrophage complement and lectin-like receptors in binding *Leishmania* parasites to host macrophages. *Immunol. Lett.* **11**, 227–232
42. Aebischer, T., Bennett, C. L., Pelizzola, M., Vizzardelli, C., Pavelka, N., Urbano, M., Capozzoli, M., Luchini, A., Ilg, T., Granucci, F., Blackburn, C. C., and Ricciardi-Castagnoli, P. (2005) A critical role for lipophosphoglycan in proinflammatory responses of dendritic cells to *Leishmania mexicana*. *Eur. J. Immunol.* **35**, 476–486
43. De Veer, M. J., Curtis, J. M., Baldwin, T. M., DiDonato, J. A., Sexton, A., McConville, M. J., Handman, E., and Schofield, L. (2003) MyD88 is essential for clearance of *Leishmania major*: possible role for lipophosphoglycan and Toll-like receptor 2 signaling. *Eur. J. Immunol.* **33**, 2822–2831
44. Becker, I., Salaiza, N., Aguirre, M., Delgado, J., Carrillo-Carrasco, N., Kobeh, L. G., Ruiz, A., Cervantes, R., Torres, A. P., Cabrera, N., Gonzalez, A., Maldonado, C., and Isibasi, A. (2003) *Leishmania* lipophosphoglycan (LPG) activates NK cells through Toll-like receptor-2. *Mol. Biochem. Parasitol.* **130**, 65–74
45. Russell, D. G., and Yates, R. M. (2007) Toll-like receptors and phagosome maturation. *Nat. Immunol.* **8**, 217–218
46. Champion, J. A., and Mitragotri, S. (2006) Role of target geometry in phagocytosis. *Proc. Natl. Acad. Sci. U. S. A.* **103**, 4930–4934
47. Henry, R. M., Hoppe, A. D., Joshi, N., and Swanson, J. A. (2004) The uniformity of phagosome maturation in macrophages. *J. Cell Biol.* **164**, 185–194
48. Lindmark, H., Rosengren, B., Hurt-Camejo, E., and Bruder, C. E. (2004) Gene expression profiling shows that macrophages derived from mouse embryonic stem cells is an improved in vitro model for studies of vascular disease. *Exp. Cell Res.* **300**, 335–344
49. Tighe, H., Corr, M., Roman, M., and Raz, E. (1998) Gene vaccination: plasmid DNA is more than just a blueprint. *Immunol. Today* **19**, 89–97
50. Schaible, U. E., Sturgill-Koszycki, S., Schlesinger, P. H., and Russell, D. G. (1998) Cytokine activation leads to acidification and increases maturation of *Mycobacterium avium*-containing phagosomes in murine macrophages. *J. Immunol.* **160**, 1290–1296
51. MacMicking, J. D., Taylor, G. A., and McKinney, J. D. (2003) Immune control of tuberculosis by IFN- γ -inducible LRG-47. *Science* **302**, 654–659
52. Alvarez-Dominguez, C., and Stahl, P. D. (1998) Interferon- γ selectively induces Rab5a synthesis and processing in mononuclear cells. *J. Biol. Chem.* **273**, 33901–33904
53. Crowley, M. T., Costello, P. S., Fitzer-Attas, C. J., Turner, M., Meng, F., Lowell, C., Tybulewicz, V. L., and DeFranco, A. L. (1997) A critical role for Syk in signal transduction and phagocytosis mediated by Fc γ receptors on macrophages. *J. Exp. Med.* **186**, 1027–1039
54. Fitzer-Attas, C. J., Lowry, M., Crowley, M. T., Finn, A. J., Meng, F., DeFranco, A. L., and Lowell, C. A. (2000) Fc γ receptor-mediated phagocytosis in macrophages lacking the Src family tyrosine kinases Hck, Fgr, and Lyn. *J. Exp. Med.* **191**, 669–682

Received for publication March 6, 2008.

Accepted for publication September 17, 2008.